29th AIAA Applied Aerodynamics Conference
27 - 30 June 2011, Honolulu, Hawaii

AIAA 2011-3509

Further Studies of Airfoils Supporting Non-unique Solutions in Transonic Flow

Antony Jameson,* John C. Vassberg, † and Kui Ou ‡

Aeronautics and Astronautics Department, Stanford University, Stanford, CA 94305

Non-unique solutions of the Euler equations were originally discussed by Jameson in 1991 for several highly cambered airfoils which were the result of aggressive shape optimization. In 1999 Hafez and Guo found non-unique solutions for a symmetric parallel sided airfoil, and subsequently Kuzmin and Ivanova have discovered some fully convex symmetric airfoils that provide non-unique solutions. In this article four new symmetric airfoils, all of which exhibit non-unique solutions in a narrow band of transonic Mach numbers, were studied. The first, NU4 was the result of shape optimization. The second, JF1 is an extremely simple parallel sided airfoil. The third JB1, is also parallel sided but has continuous curvature over the entire profile. The fourth, JC6, is convex and C_∞ continuous. $C_L - \alpha$ plots of these airfoils exhibit three branches of zero angle of attack, the P, Z and N-branches with positive, zero and negative lift respectively. At some Mach numbers no stable Z-branch could be found. When the P-branch is continued to negative α in some cases there is a transition to the Z-branch, while in other cases there is a direct transition from the P to N-branch.

I. Introduction

Given that the equations governing steady inviscid compressible flow are nonlinear, one can anticipate the possibility of non-unique solutions. A familiar example is the case of supersonic flow past a wedge at an angle θ, where there are two solutions with different shock angles β corresponding to the strong and weak branches of the $\beta-\theta$ diagram. Non-unique solutions of the transonic potential flow equation were discovered by Steinhoff and Jameson[1] (1981), who obtained lifting solutions for a symmetric Joukowski airfoil at zero angle of attack in a narrow range of Mach numbers in the neighborhood of Mach 0.85. This non-uniqueness could not be duplicated with the Euler equations and it was conjectured by Salas et al[2] (1983) that the non-uniqueness was a consequence of the isentropic flow approximation. Subsequently, however, Jameson[3] (1991) discovered several airfoils which supported non-unique solutions of the Euler equations in a narrow Mach band. These airfoils were lifting.

The question of non-unique transonic flows was re-examined by Hafez and Guo[4–6] (1999) who formed both lifting and non-lifting solutions for a 12 percent thick symmetric airfoil with parallel sides from 25 to 75 percent chord in a Mach range from 0.825 to 0.843. The question was further pursued in detail in a series of studies by Kuz'min and Ivanova[7–11] (2004,2006) who confirmed the results of Hafez and Guo, and also showed that airfoils with positive curvature everywhere could support non-unique solutions.

II. Problem Statement

II.A. NU4 Airfoil

The present authors have encountered another example as a consequence of a shape optimization study for symmetric airfoils in transonic flow,[12] in which an attempt was made to find a 12 percent thick airfoil with a shock free solution at Mach 0.84. The resulting airfoil, labelled NU4, has an almost shock free solution at its design Mach number, but also allows a lifting and non-lifting solution at zero angle of attack. In order

*Thomas V Jones Professor, Aeronautics and Astronautics Department, Stanford University, AIAA Fellow.
†Boeing Technical Fellow, The Boeing Company, AIAA Fellow.
‡PhD Candidate, Aeronautics and Astronautics Department, Stanford University, AIAA Student Member.

to better understand this phenomenon three other ~ 12 percent thick symmetric airfoils have been analyzed in detail.

II.B. JF1 Airfoil

The first, JF1 airfoil, is even simpler than the shape proposed by Hafez and Guo, consisting of a parallel sided slab closed by a semi-circular nose and two parabolic arcs at the rear. Depending on the extent of the parabolic arcs a Mach range exists in which lifting solutions can be found at zero angle of attack.

II.C. JB1 Airfoil

The second, JB1 airfoil, also has a parallel center section but the nose and tail are closed by higher order curves which maintain continuity of the curvature at the junction points. The nose section is defined by a Bezier curve with the control points

$$x_1 = 0, y_1 = 0$$
$$x_2 = 0, y_2 = 1$$
$$x_3 = 1, y_3 = 1$$
$$x_4 = 1, y_4 = 1$$

scaled to a length of .125 and a height of .0625. The upper surface curve is defined by

$$\begin{array}{c} x = .125(3t^2 - 2t^3) \\ y = .0625(3t - 3t^2 + t^3) \end{array} , \ 0 \le t \le 1$$

The trailing curve from $x = .625$ to 1 is

$$y = .0625 \left[1 - \left(1 - \left(\frac{1-x}{.375} \right) \right)^3 \right]$$

II.D. JC6 Airfoil

The third airfoil, JC6, is a fully convex airfoil defined by a simple algebraic formula

$$y(x) = Cx^{\frac{1}{n}}(1 - x^n), 0 \le x \le 1$$

where the constant C, with a value of 0.06817, is adjusted to give the specified maximum thickness, 12 percent of the chord. The choice n=6 results in a very blunt-nosed airfoil with maximum thickness at about 55 percent of the chord, which has positive curvature everywhere and is C_∞ continuous.

II.E. Overview

These four airfoils have very different characteristics, but they all share the property that in non-lifting transonic flow they exhibit a transition from a solution with two supersonic zones on each surface below a certain critical Mach number to a situation with one supersonic zone on each surface above the critical Mach number. In the region of instability solutions with positive lift are found in which there is a single supersonic zone on the top surface and two supersonic zones on the lower surface, and also solutions with negative lift which are the mirror images of the solutions with positive lift. There results are presented in more detail below.

III. Results

The calculations for the first three airfoils were performed using the authors' SYN83 code, which implements the Jameson-Schmidt-Turkel scheme[13] on a mesh with C-topology. The mesh contained 384 cells in the clockwise direction and 64 cells in the normal direction.

III.A. NU4 Airfoil

Examining first the NU4 airfoil stable asymmetric solutions were found in the range of Mach numbers from 0.837 to 0.841. As the Mach number is increased there is again a progressively decreasing distance between the two supersonic zones on the lower surface (in the case of positive lift). This is illustrated in Figures (1) to (3). At Mach 0.841 the symmetric solution is close to shock free, with a single relatively weak shock.

III.B. JF1 Airfoil

Examining next the JF1 airfoil, closed at the rear by parabolic arcs from 76 percent chord, non-unique solutions are found in the range of Mach numbers from 0.825 to 0.835, illustrated in Figures (4) to (6). Figures (4)(a) and (4)(c) show the symmetric and positive lifting solutions at Mach 0.825 respectively, together with their convergence histories. The lifting solution was obtained by starting at an angle of attack of 0.005 degrees, and switching to zero after 500 iterations. The corresponding negative lifting solution can be obtained by starting at -0.005 degrees, and is the exact mirror image. Figures (5) and (6) show the corresponding results at Mach 0.830 and 0.835. As the Mach number is increased the double shock zone becomes narrower. When it becomes too narrow above Mach 0.835 or too wide below Mach 0.825 the initial lifting solution at 0.005 degrees decays when the angle of attack is reduced to zero. It may also be observed that the symmetric solutions at Mach 0.825 and 0.830 started to diverge after reaching extremely low values of the residual of the order of 10^{-12} and 10^{-11} respectively at around 1500 cycles, suggesting that at these Mach numbers the symmetric solution may not be a stable equilibrium point. Syn83 uses a multigrid solution procedure, in combination with variable local time steps and residual averaging. These procedures could possibily stabilize an unstable solution, so time accurate simulations will be needed to assess the true stability of the symmetric solutions.

III.C. JB1 Airfoil

The JB1 airfoil differs from the JF1 airfoil primarily in maintaining continuity of the curvature over the entire profile, and having a slightly larger thickness of 12.5 percent. Nevertheless the results displayed in Figure (7) - (15) have a very similar character, with non-unique solutions in a somewhat narrower range of Mach numbers from .823 to .827.

III.D. JC6 Airfoil

Corresponding results for the JC6 airfoil are shown in Figures (10) to (12). In these cases stable asymmetric solutions are formed in the range of Mach numbers from 0.844 to 0.848. These calculations were also performed with Syn83, but because of the extreme blunt nose shape of this airfoil, a finer mesh with 768x128 cells was used. The general characters of the solutions is externally similar to that of the JF1 airfoils, confirming that non-unique solutions can be found for an extremely smooth convex profile with positive curvature everywhere. In order to verify that these solutions are not a consequence of the mesh or the discretization scheme, this airfoil has also ben analyzed on an O-mesh with 512x512 cells with an uniform aspect ratio of unity. Figure (13) illustrates a corresponding mesh with 128x128 cells. Calculations were performed using a version of the authors' FLO82 code which implements the H-CUSP scheme,[14] and with NASA's Overflow code.[15] The results confirmed the same trend. Figure (14) shows the three solutions for Mach .847 at zero angle of attack calculated using FLO82.

III.E. Plots of $C_L - \alpha$ Sweeps

In order to further elucidate the behavior C_L vs α curves have been calculated for all four airfoils at Mach number where they exhibit non-unique solutions. Overall three different regimes can be identified as the Mach number is varied over a narrow band. Typically the $C_L - \alpha$ curve has three branches with zero, positive and negative lift at zero angle of attack (the Z, P and N branches). In the first regime there appears to be no stable solution at zero angle of attack although it may be possible to force convergence to very small values of the error residual. In this case there is no Z-branch. The P-branch can be continued to negative angles of attack before there is a transition directly to the N-branch. In the second regime there is a Z-branch in which stable solutions are found over a small range of angle of attack. However, when the P-branch is continued to negative α there is eventually a direct transition to the N-branch. In the third regime there is

a larger Z-branch, and when the P-branch is continued to negative α there is a transition to the Z-branch, and then as α is further reduced to more negative value there is a second transition to the N-branch. These regimes can be seen for the different airfoils in Figures (15) - (18). Figure (15) shows the NU4 airfoil at Mach .840. It exhibits the third behavior with transition from the P to the N-branch via the Z-branch. Figure (16) shows that the JF1 airfoil has a similar behavior at Mach .835. the lower figure is a zoom of the upper picture. Figure (17) shows the JB1 airfoil at Mach .827. This shows the second regime where there is a direct transition from the P to the N-branch. At Mach .825 no stable Z-branch could be found for this airfoil, indicating that it is in the first regime. Figure (18) shows that the JC6 airfoil is in the second regime at Mach .847. In this case the $C_L - \alpha$ sweep was calculated on 512×512 O-mesh using both FLO82-HCUSP and Overflow, in order to verify the behavior.

IV. Conclusion

The results for these four very different airfoils exhibit a similar general pattern. They all have solutions which have a rather abrupt transition from two supersonic zones below a certain critical Mach number to a single supersonic zone above that Mach number. Non-uniqueness occurs in a range of Mach numbers between a point at which the two zones are quite widely spaced up to the point at which they coalesce. In this range symmetric double shocked solutions appear to be unstable. Stable asymmetric solutions are found when two supersonic zones coalesce on one surface but not the other. When, for example, there are two supersonic zones on the lower surface the increase in pressure behind the first shock produces lift. The corresponding circulation then leads to an increase in the effective Mach number on the upper surface and a decrease on the lower surface, thus reinforcing the upper and lower surface solutions along the branches corresponding to single and double supersonic zones respectively. This mechanism is not sufficient, however, to describe the behaviors of the original non-unique solutions for lifting airfoils reported by Jameson in 1991. Unsteady simulations similar to those performed by Caughey[16] (2004) are needed to gain a better understanding of the evolution and stability of these flows.

References

[1]J. Steinhoff, and A. Jameson, *Multiple solution of the transonic potential flow equations*, AIAA J. 20(11), 15211525 (1982)

[2]M.D. Salas, R.E. Melnik, and A. Jameson, *A comparative study of the non-uniqueness problem of the potential equation*, AIAA Paper 83-1888, (1983)

[3]A. Jameson, *Airfoil admitting non-unique solutions to the Euler equations*, AIAA Paper 91-1625 (1991)

[4]M.M. Hafez and W.H. Guo, *Nonuniqueness of transonic ows*, Acta Mech. 138, 177184 (1999a)

[5]M.M. Hafez and W.H. Guo, *Some anomalies of numerical simulation of shock waves*, Part I: inviscid ows. Comput. Fluids 28(45), 701719 (1999b)

[6]M.M. Hafez and W.H. Guo, *Some anomalies of numerical simulation of shock waves. Part II: effect of articial and real viscosity*, Comput. Fluids 28(45), 721739 (1999c)

[7]A.G. Kuzmin and A.V. Ivanova, *The structural instability of transonic flow associated with amalgamation/splitting of supersonic regions*, Theoret. Comput. Fluid Dynamics (2004) 18:335-344

[8]A.G. Kuzmin, *Instability and bifurcation of transonic flow over airfoils*, AIAA Paper, 2004

[9]A.V. Ivanova and A.G. Kuzmin, *Non-uniqueness of the transonic flow past an airfoil*, Fluid Dynamics, Vol. 39, No.4, pp.642-648, (2004)

[10]A.G. Kuzmin, *Bifurcation of transonic flow over a flattened airfoil*, Frontiers of Computational Fluid Dynamics, World Scientific Publishing Company LTD, (2006)

[11]Kuzmin, *Structural instability of transonic flow over an airfoil*, Journal of Engineering Physics and Thermophysics, Vol. 77, No.5, pp.1022-1026, (2004)

[12]J. C. Vassberg, N. A. Harrison, D. L. Roman and A. Jameson, *Systematic Study on the Impact of Dimensionality for a Two-Dimensional Aerodynamic Optimization Model Problem*, 29^{th} AIAA Applied Aerodynamics Conference, Honolulu, HI, June, 2011

[13]A. Jameson, W. Schmidt, and E. Turkel, *Numerical Solutions of the Euler Equations by Finite Volume Methods Using Runge-Kutta Time-Stepping Schemes*, AIAA Paper 81-1259, AIAA 14th Fluid and Plasma Dynamic Conference, Palo Alto, (1981)

[14]A. Jameson, *Analysis and Design of Numerical Schemes for Gas Dynamics 2 Artificial Diffusion and Discrete Shock Structure*, International Journal of Computational Fluid Dynamics, Vol. 5, 1995, pp. 1-38.

[15]P. G. Buning, D. C. Jespersen, T. H. Pulliam, G. H. Klopfer, W. M. Chan, J. P. Slotnick, S. E. Krist and K. J. Renze, *OVERFLOW User's Manual, Version 1.8L*, NASA, July, 1999

[16]D.A. Caughey, *Stability of unsteady flow past airfoils exhibiting transonic non-uniqueness*, CFD Journal 13(3):60, (2004)

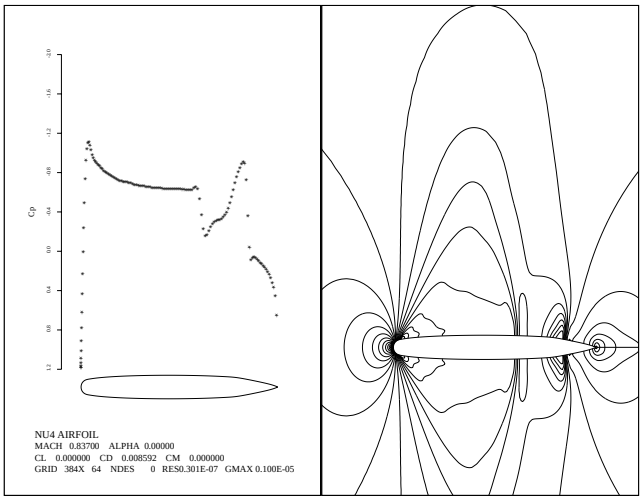

(a) Z-branch Cp Distribution and Mach Contours

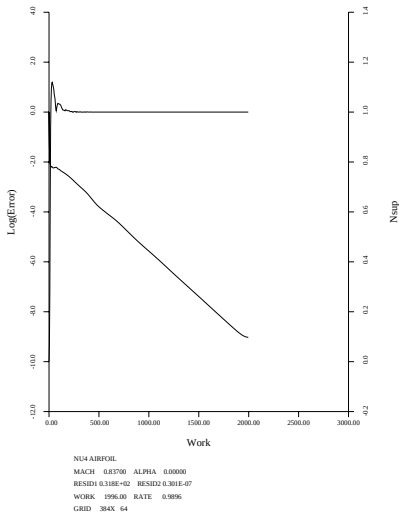

(b) Z-branch Convergence History

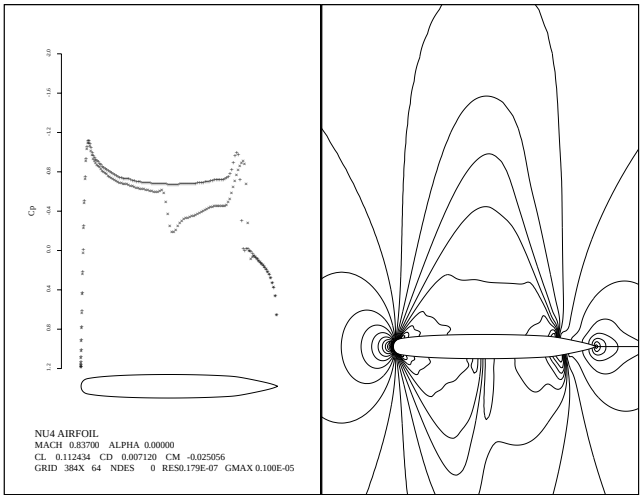

(c) P-branch Cp Distribution and Mach Contours

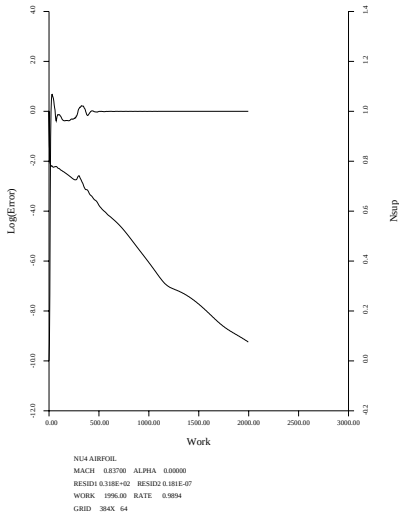

(d) P-branch Convergence History

Figure 1. NU4 at Mach=0.837 showing the symmetric solution (a) and convergence history (b), and the asymmetric solution (c) and convergence history (d)

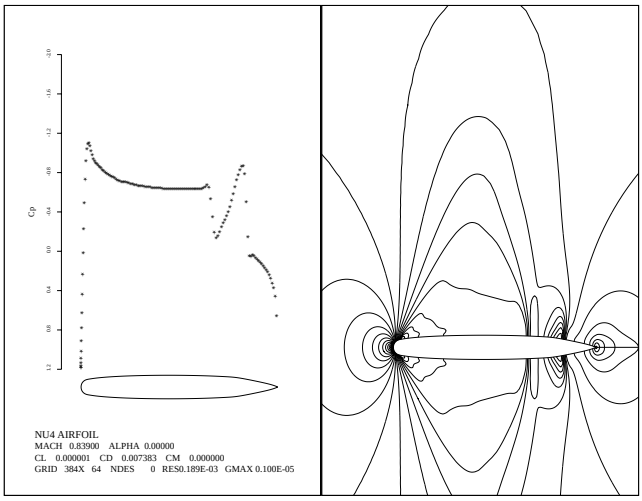

(a) Z-branch Cp Distribution and Mach Contours

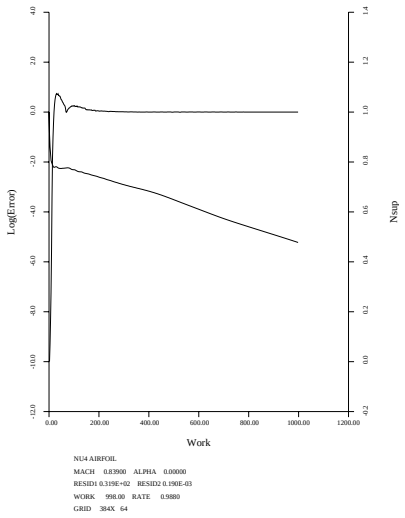

(b) Z-branch Convergence History

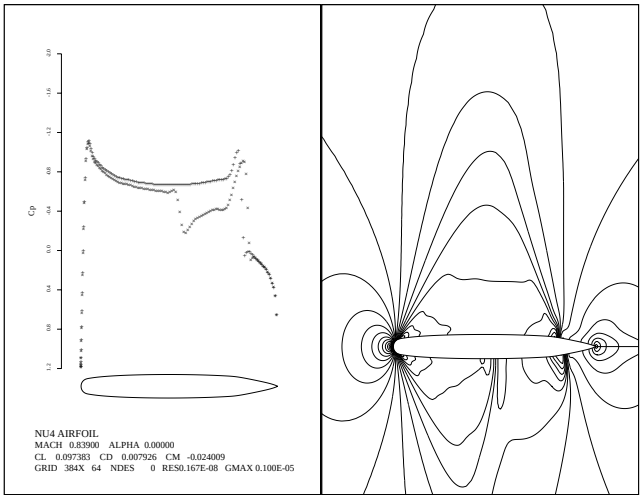

(c) P-branch Cp Distribution and Mach Contours

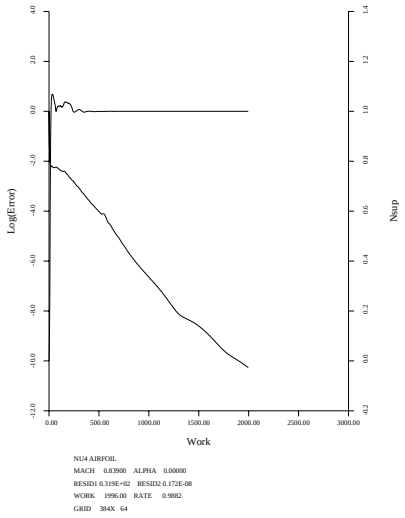

(d) P-branch Convergence History

Figure 2. NU4 at Mach=0.839 showing the symmetric solution (a) and convergence history (b), and the asymmetric solution (c) and convergence history (d)

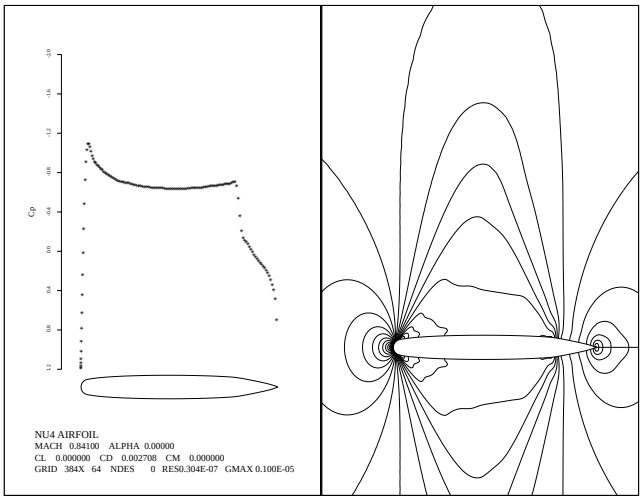

(a) Z-branch Cp Distribution and Mach Contours

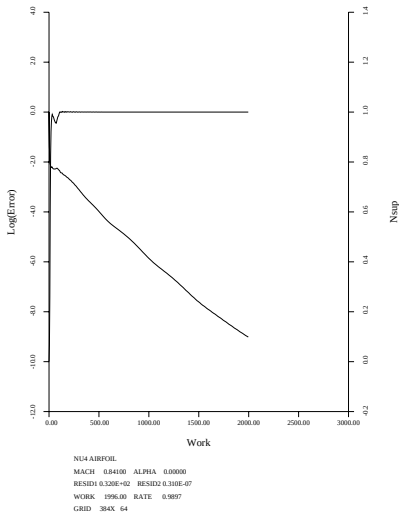

(b) Z-branch Convergence History

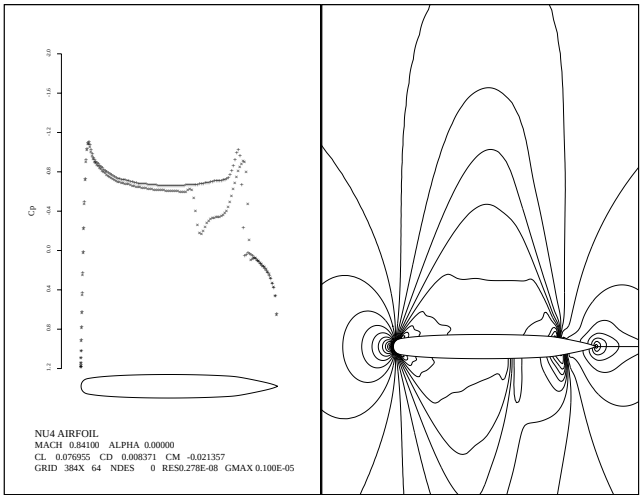

(c) P-branch Cp Distribution and Mach Contours

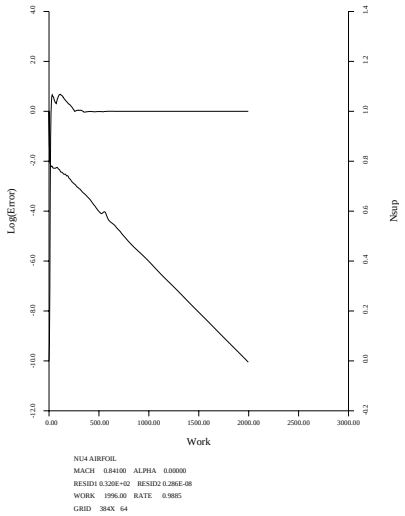

(d) P-branch Convergence History

Figure 3. NU4 at Mach=0.841 showing the symmetric solution (a) and convergence history (b), and the asymmetric solutions (c) and convergence history (d)

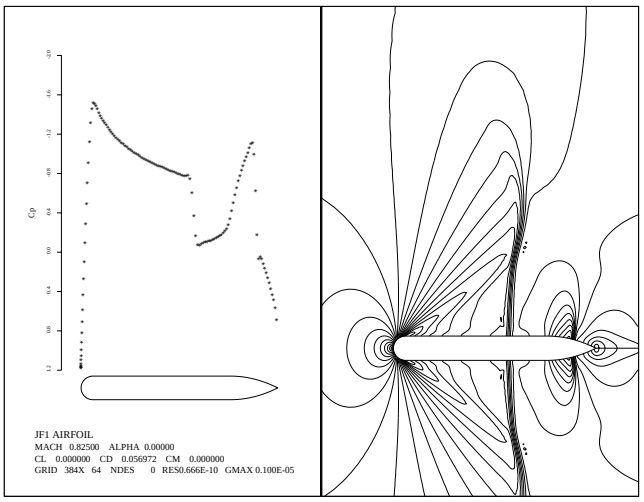

(a) Z-branch Cp Distribution and Mach Contours

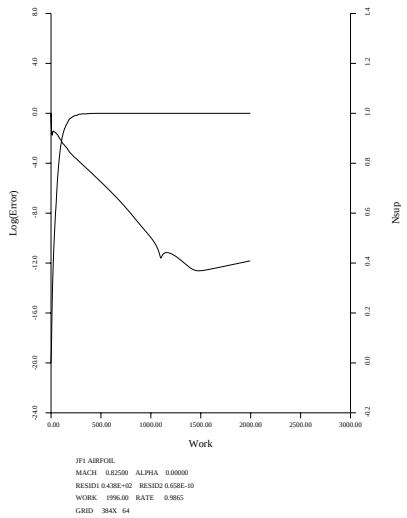

(b) Z-branch Convergence History

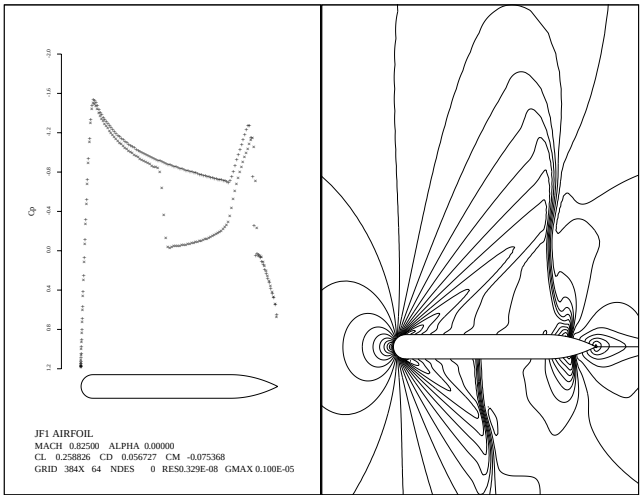

(c) P-branch Cp Distribution and Mach Contours

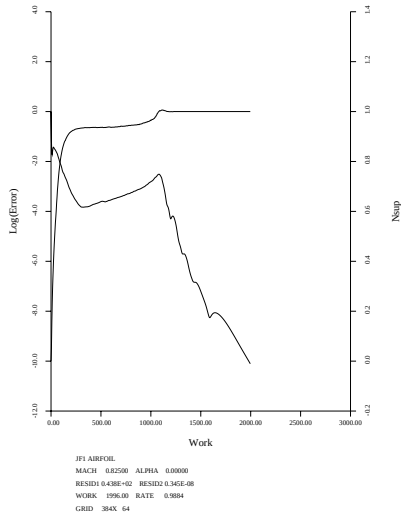

(d) P-branch Convergence History

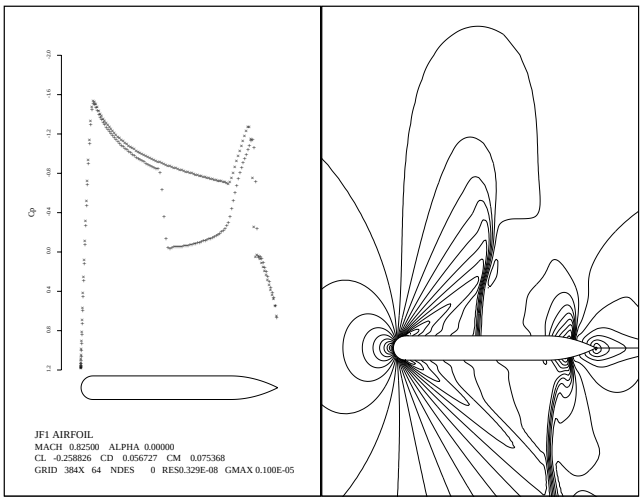

(e) N-branch Cp Distribution and Mach Contours

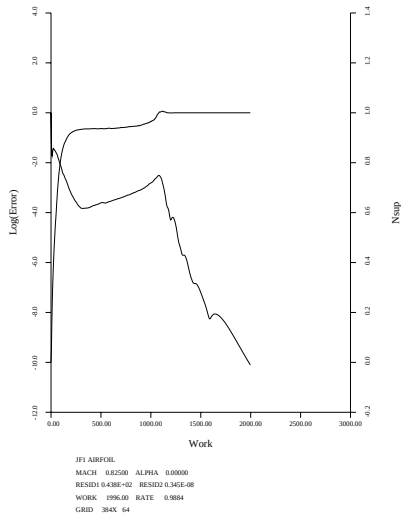

(f) N-branch Convergence History

Figure 4. JF1 at Mach=0.825 showing the symmetric solution (a) and convergence history (b), and the pair of asymmetric solutions (c)(e) and convergence histories (d)(f)

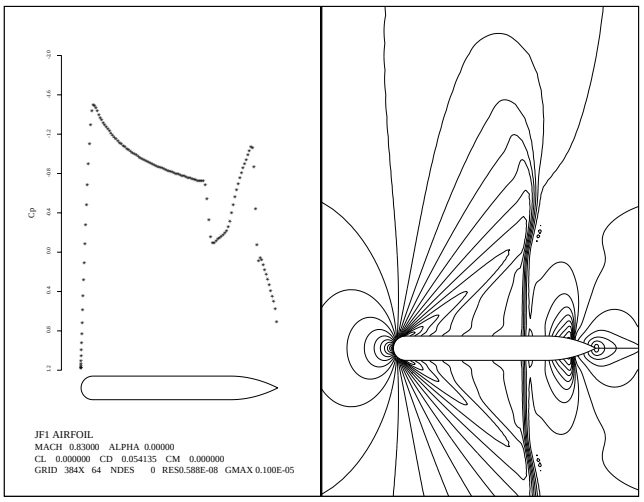

(a) Z-branch Cp Distribution and Mach Contours

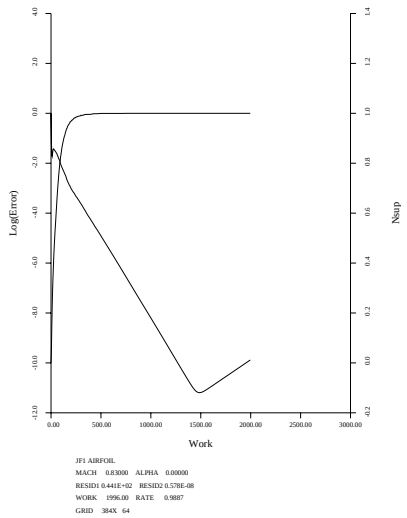

(b) Z-branch Convergence History

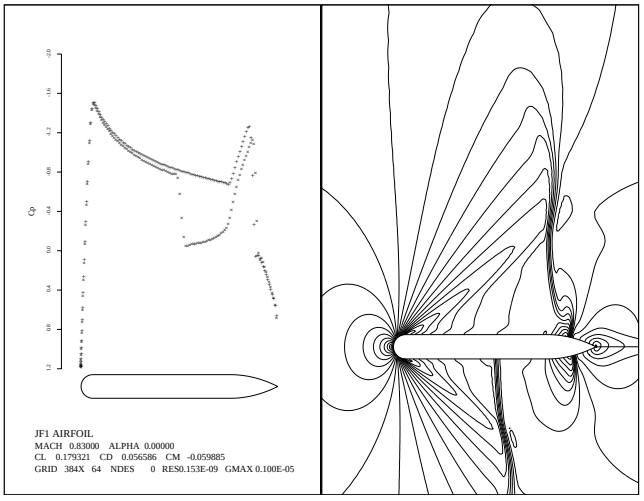

(c) P-branch Cp Distribution and Mach Contours

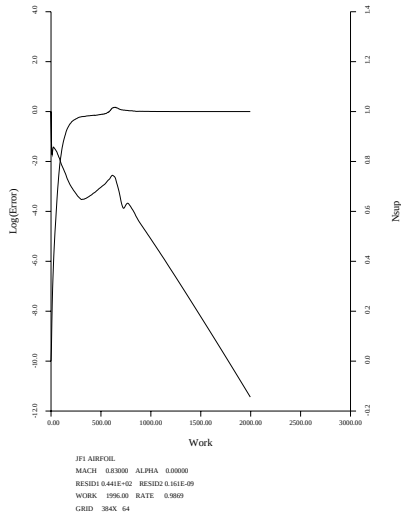

(d) P-branch Convergence History

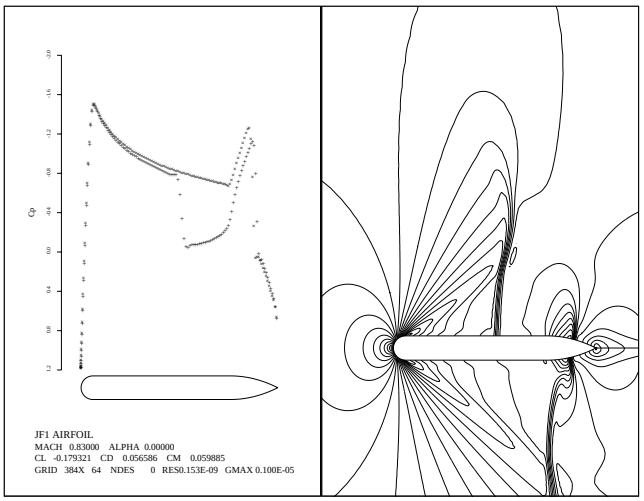

(e) N-branch Cp Distribution and Mach Contours

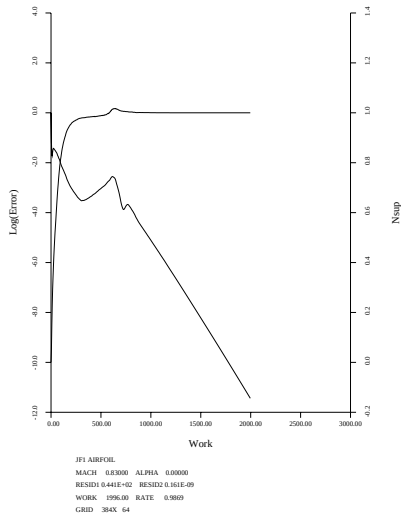

(f) N-branch Convergence History

Figure 5. JF1 at Mach=0.830 showing the symmetric solution (a) and convergence history (b), and the pair of asymmetric solutions (c)(e) and convergence histories (d)(f)

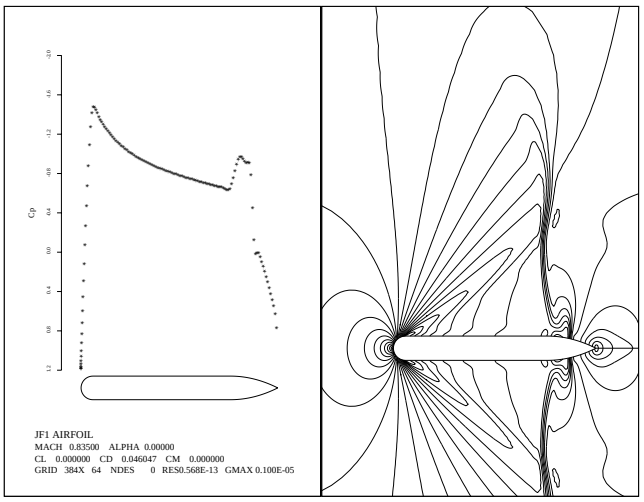

(a) Z-branch Cp Distribution and Mach Contours

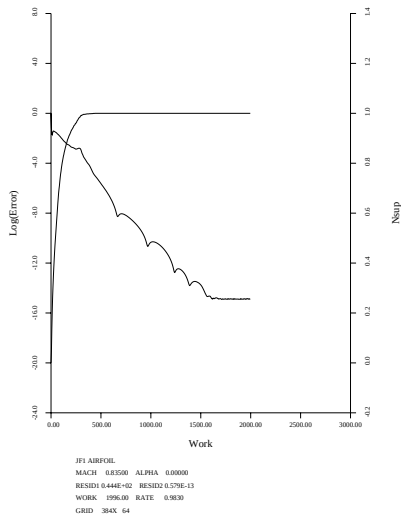

(b) Z-branch Convergence History

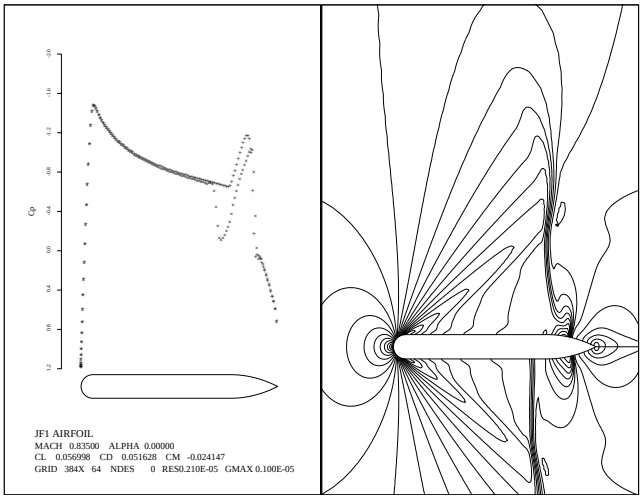

(c) P-branch Cp Distribution and Mach Contours

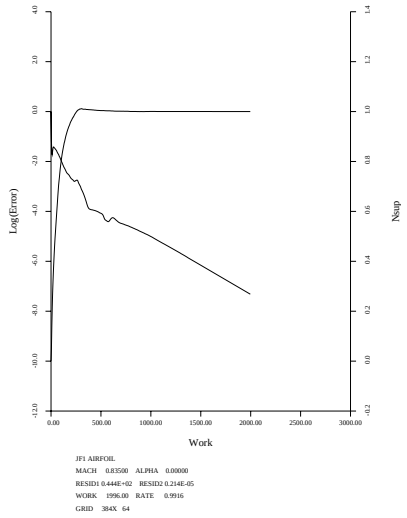

(d) P-branch Convergence History

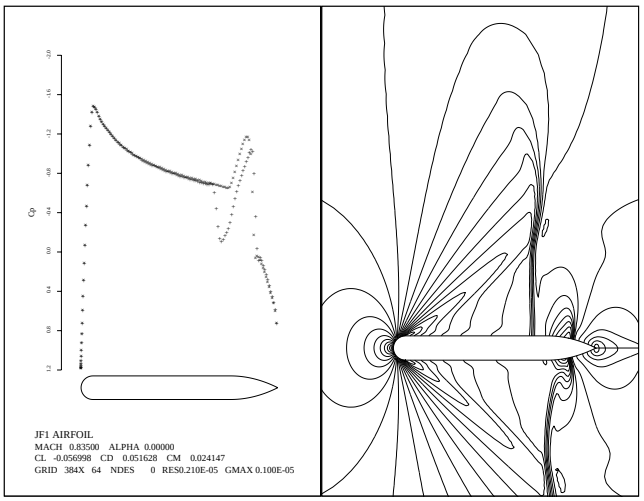

(e) N-branch Cp Distribution and Mach Contours

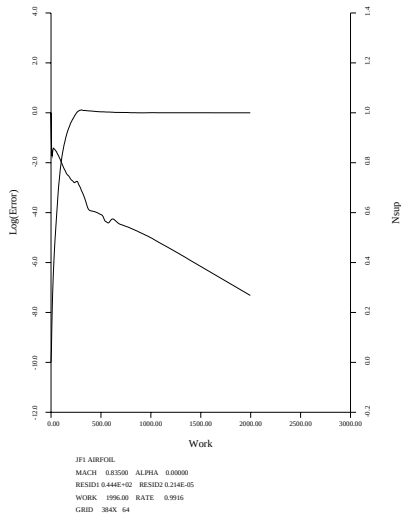

(f) N-branch Convergence History

Figure 6. JF1 at Mach=0.835 showing the symmetric solution (a) and convergence history (b), and the pair of asymmetric solutions (c)(e) and convergence histories (d)(f)

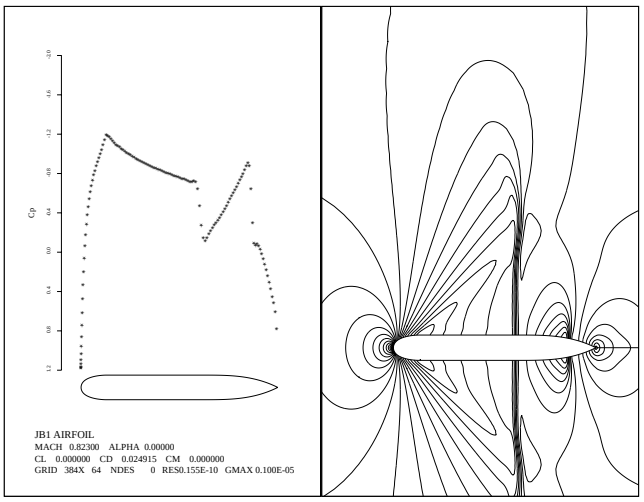

(a) Z-branch Cp Distribution and Mach Contours

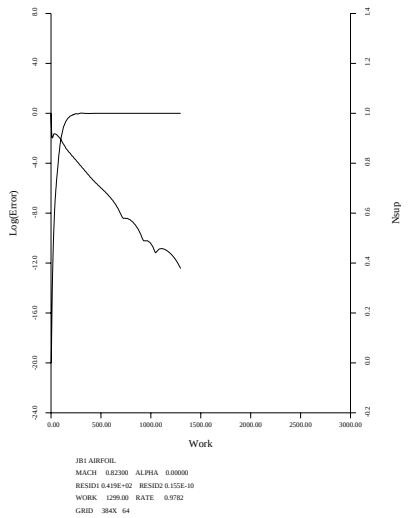

(b) Z-branch Convergence History

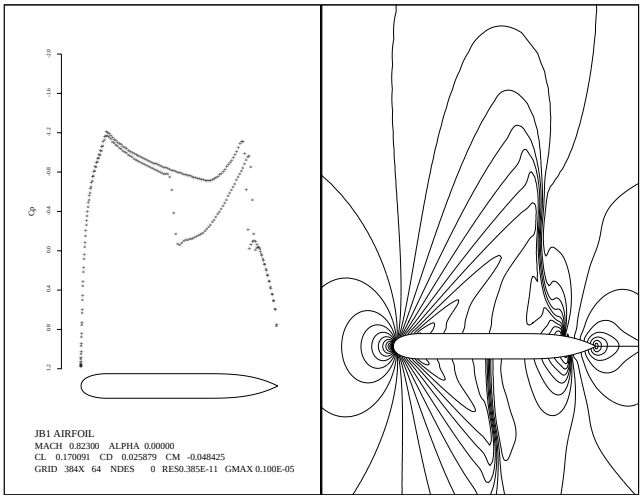

(c) P-branch Cp Distribution and Mach Contours

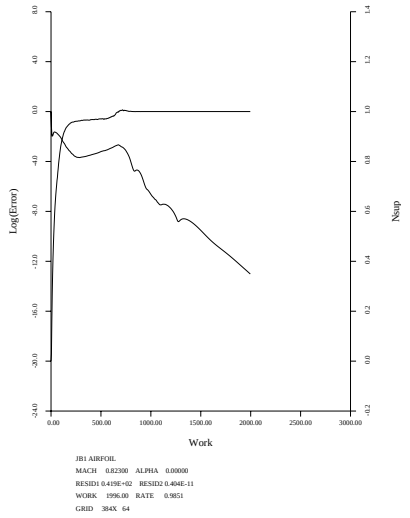

(d) P-branch Convergence History

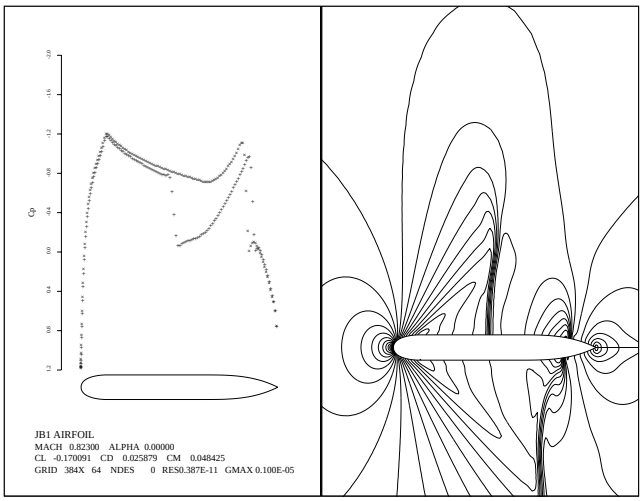

(e) N-branch Cp Distribution and Mach Contours

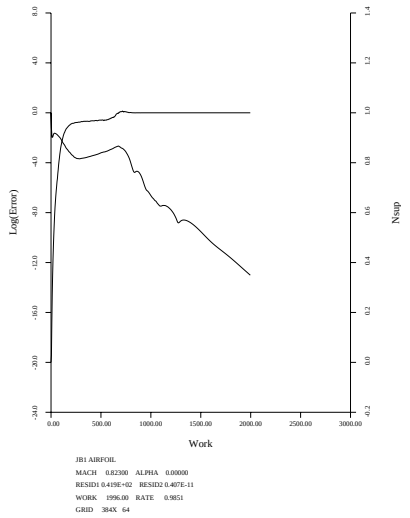

(f) N-branch Convergence History

Figure 7. JB1 at Mach=0.823 showing the symmetric solution (a) and convergence history (b), and the pair of asymmetric solutions (c)(e) and convergence histories (d)(f)

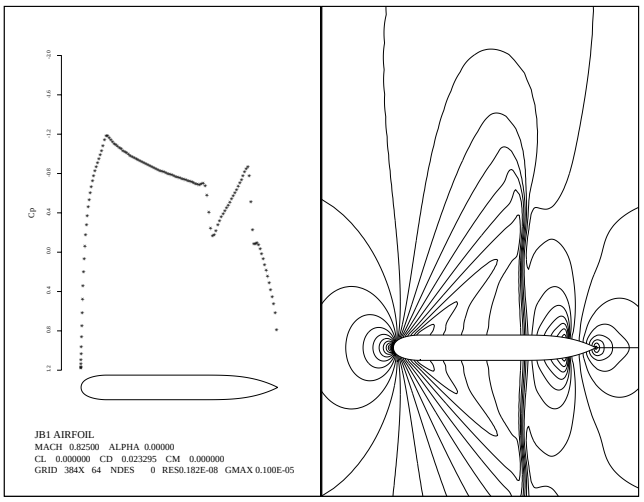

(a) Z-branch Cp Distribution and Mach Contours

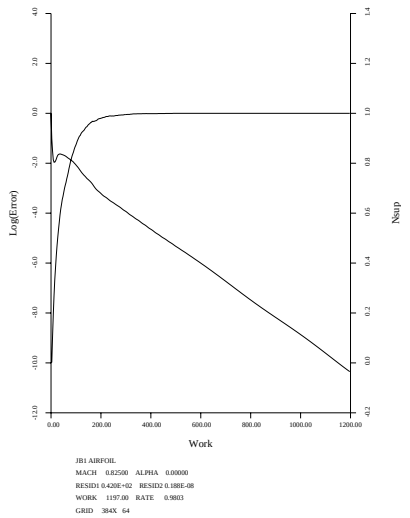

(b) Z-branch Convergence History

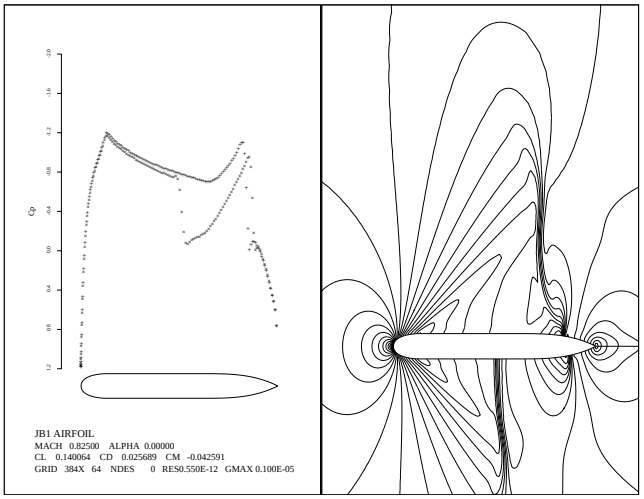

(c) P-branch Cp Distribution and Mach Contours

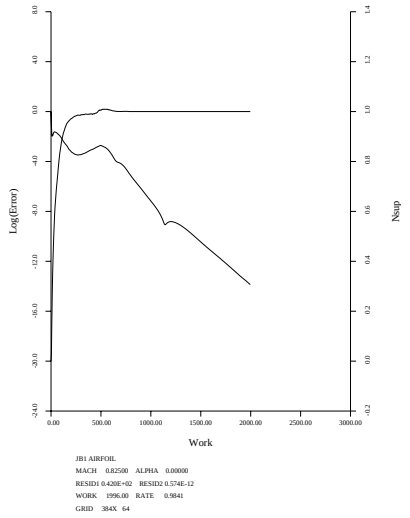

(d) P-branch Convergence History

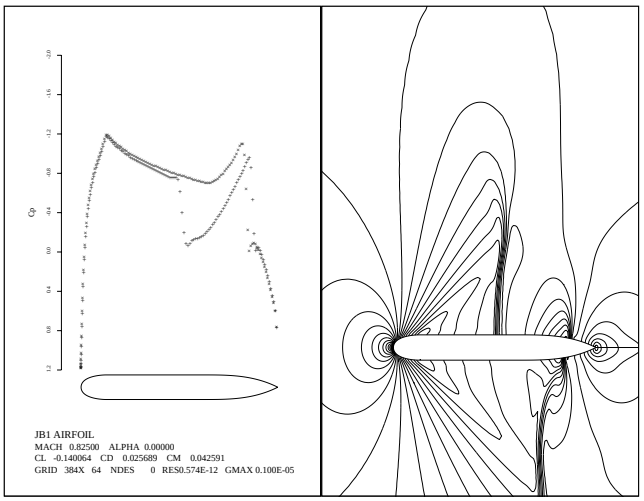

(e) N-branch Cp Distribution and Mach Contours

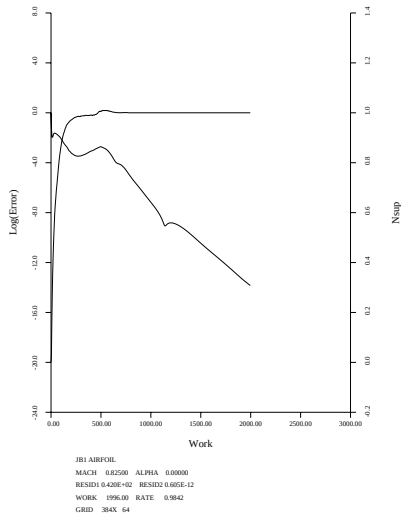

(f) N-branch Convergence History

Figure 8. JB1 at Mach=0.825 showing the symmetric solution (a) and convergence history (b), and the pair of asymmetric solutions (c)(e) and convergence histories (d)(f)

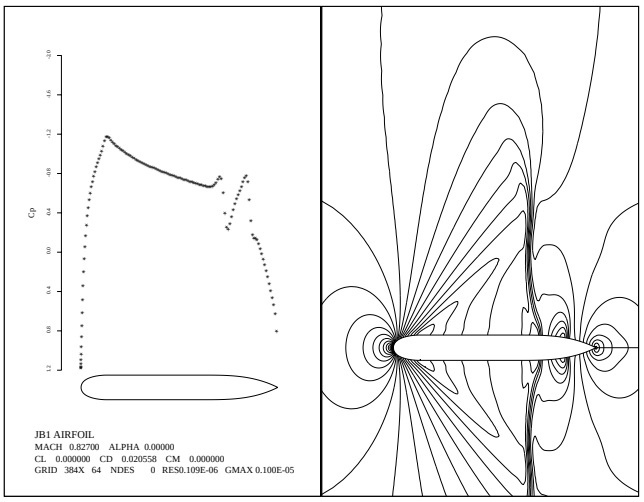

(a) Z-branch Cp Distribution and Mach Contours

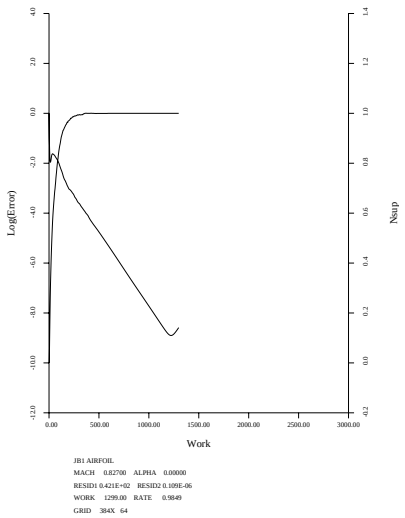

(b) Z-branch Convergence History

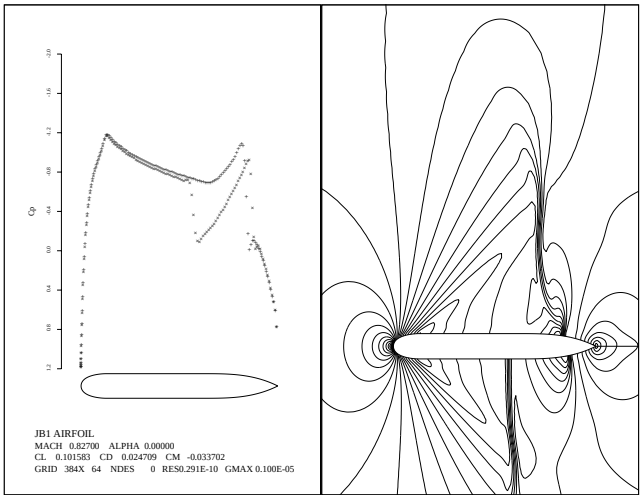

(c) P-branch Cp Distribution and Mach Contours

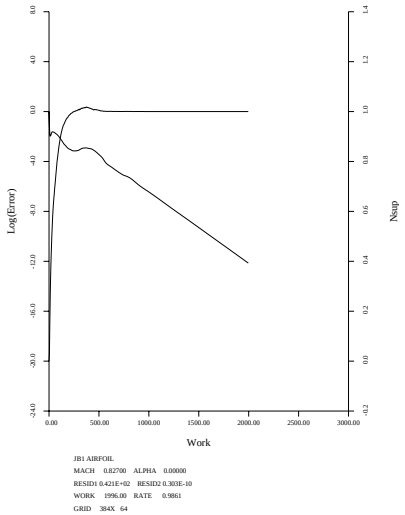

(d) P-branch Convergence History

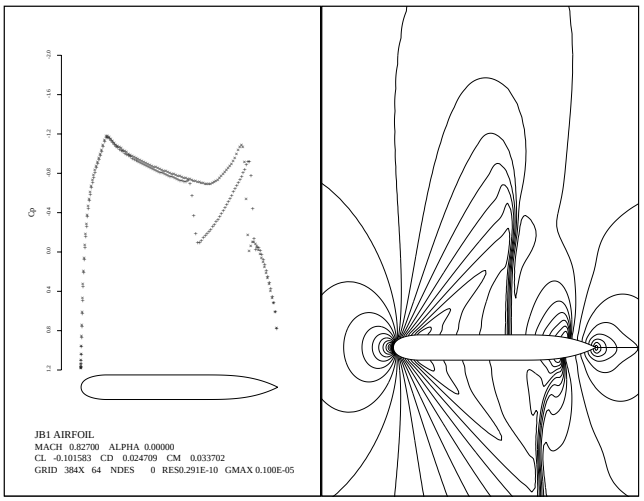

(e) N-branch Cp Distribution and Mach Contours

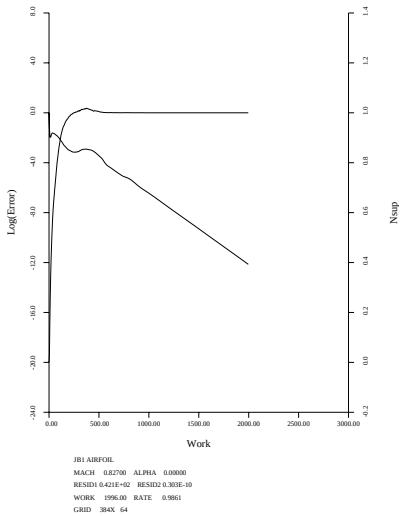

(f) N-branch Convergence History

Figure 9. JB1 at Mach=0.827 showing the symmetric solution (a) and convergence history (b), and the pair of asymmetric solutions (c)(e) and convergence histories (d)(f)

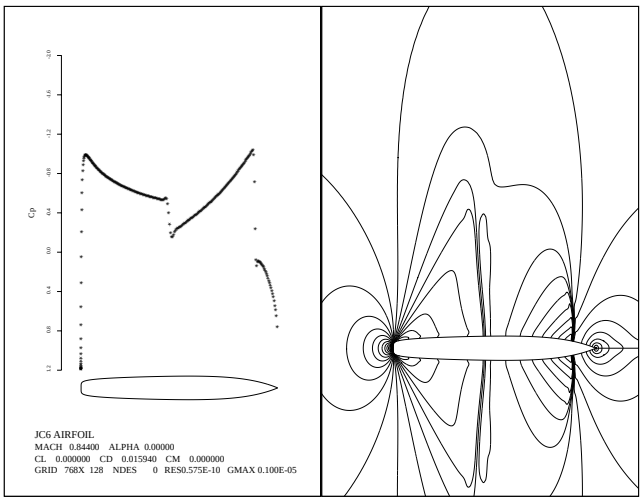

(a) Z-branch Cp Distribution and Mach Contours

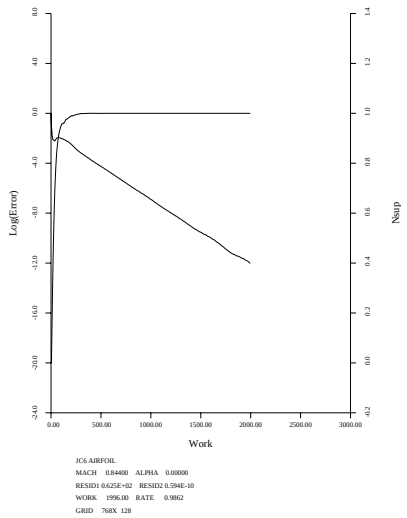

(b) Z-branch Convergence History

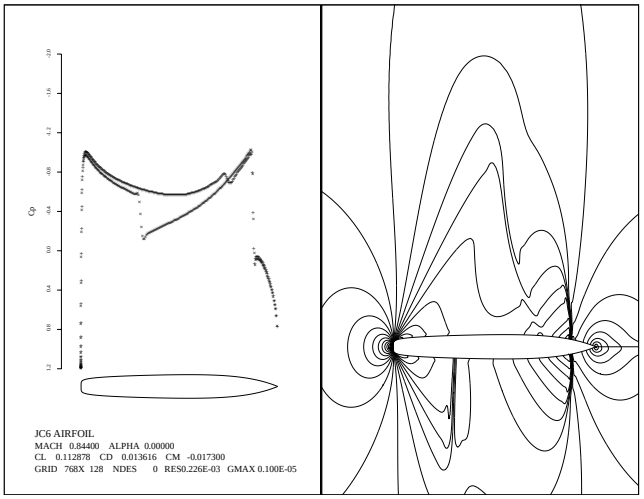

(c) P-branch Cp Distribution and Mach Contours

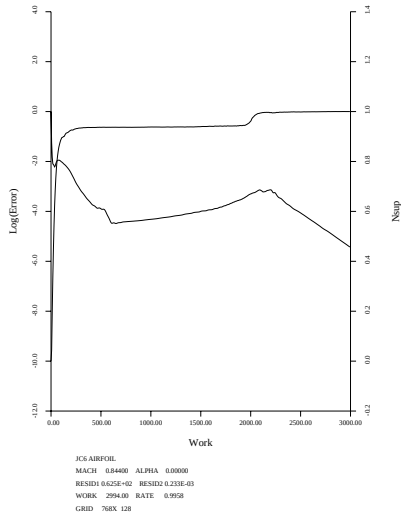

(d) P-branch Convergence History

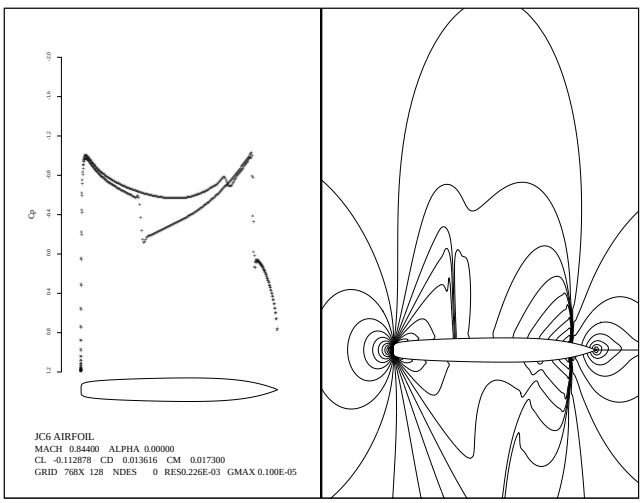

(e) N-branch Cp Distribution and Mach Contours

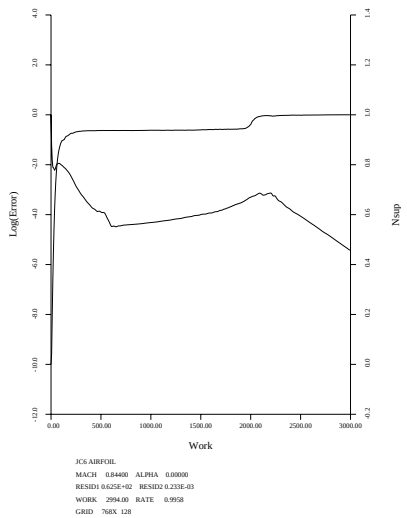

(f) N-branch Convergence History

Figure 10. JC6 at Mach=0.844 showing the symmetric solution (a) and convergence history (b), and the pair of asymmetric solutions (c)(e) and convergence histories (d)(f)

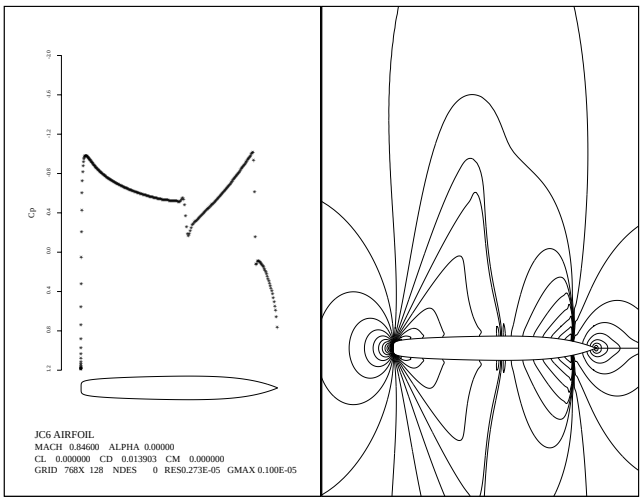

(a) Z-branch Cp Distribution and Mach Contours

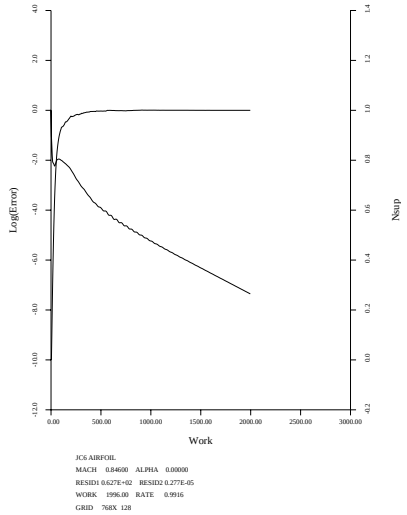

(b) Z-branch Convergence History

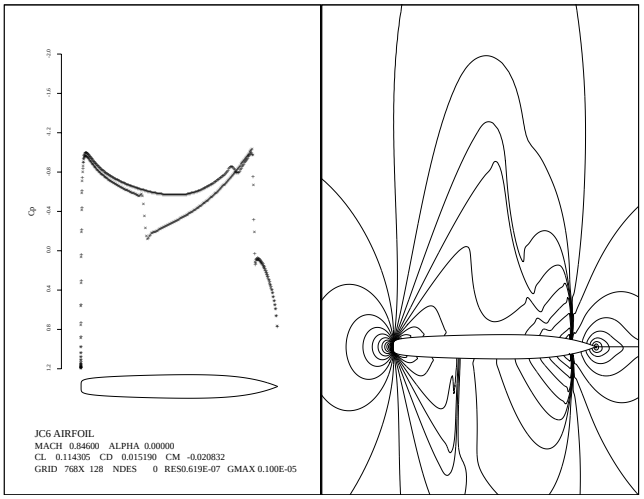

(c) P-branch Cp Distribution and Mach Contours

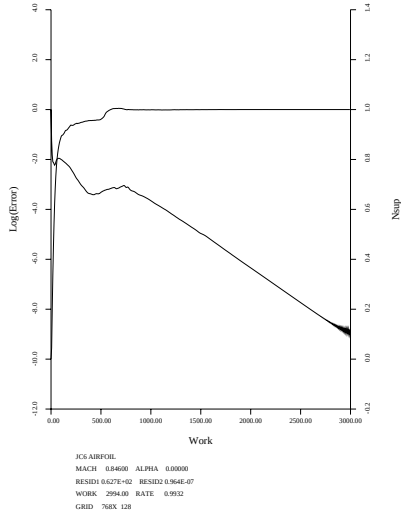

(d) P-branch Convergence History

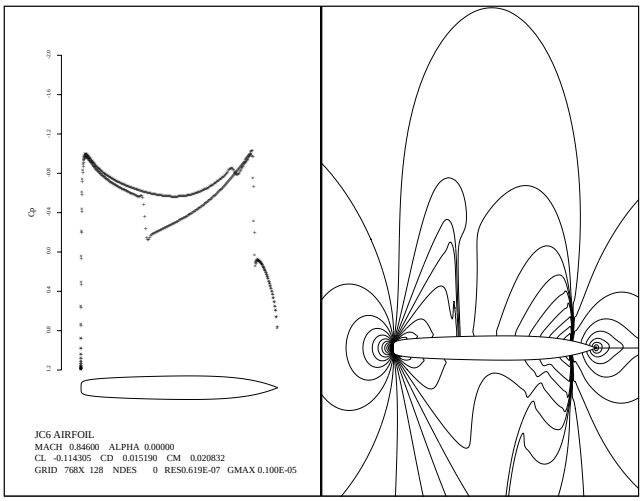

(e) N-branch Cp Distribution and Mach Contours

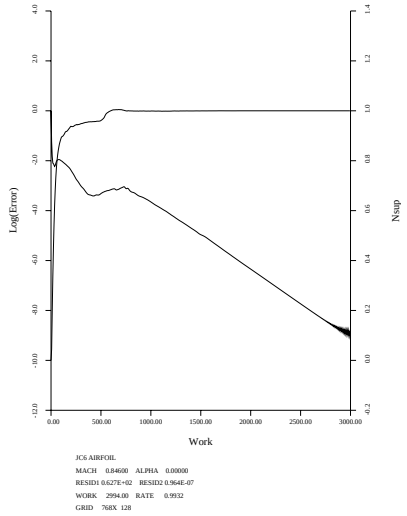

(f) N-branch Convergence History

Figure 11. JC6 at Mach=0.846 showing the symmetric solution (a) and convergence history (b), and the pair of asymmetric solutions (c)(e) and convergence histories (d)(f)

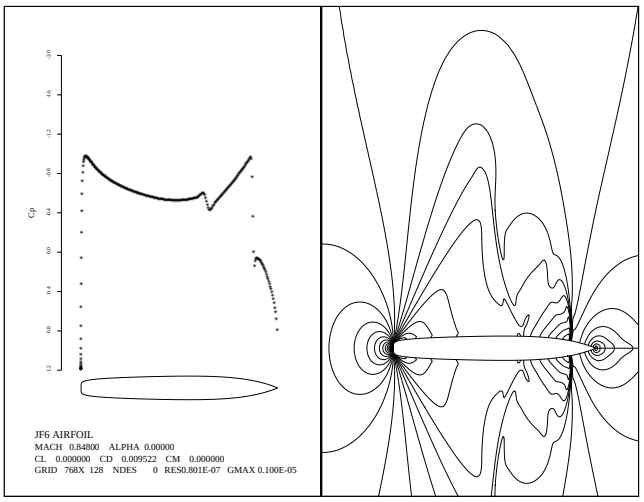

(a) Z-branch Cp Distribution and Mach Contours

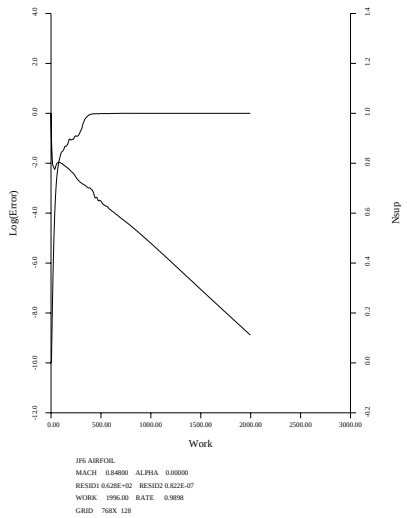

(b) Z-branch Convergence History

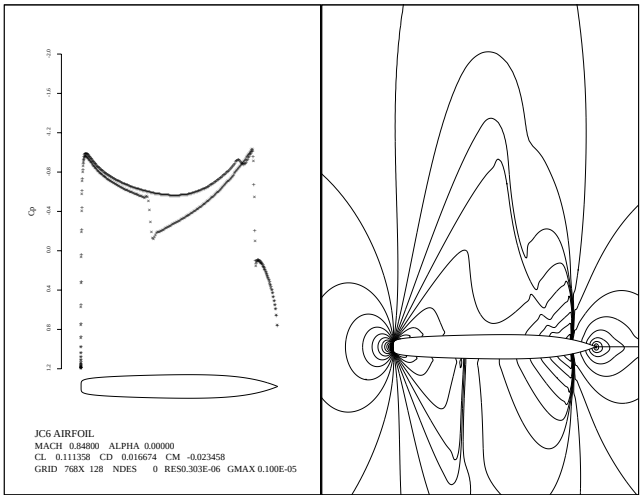

(c) P-branch Cp Distribution and Mach Contours

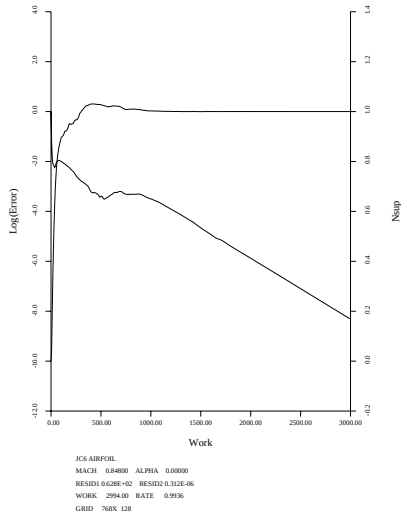

(d) P-branch Convergence History

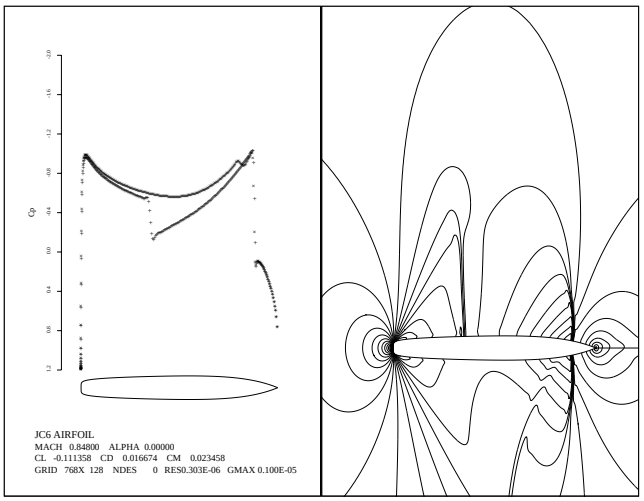

(e) N-branch Cp Distribution and Mach Contours

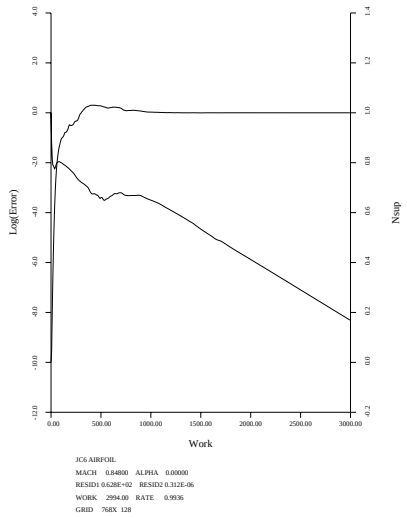

(f) N-branch Convergence History

Figure 12. JC6 at Mach=0.848 showing the symmetric solution (a) and convergence history (b), and the pair of asymmetric solutions (c)(e) and convergence histories (d)(f)

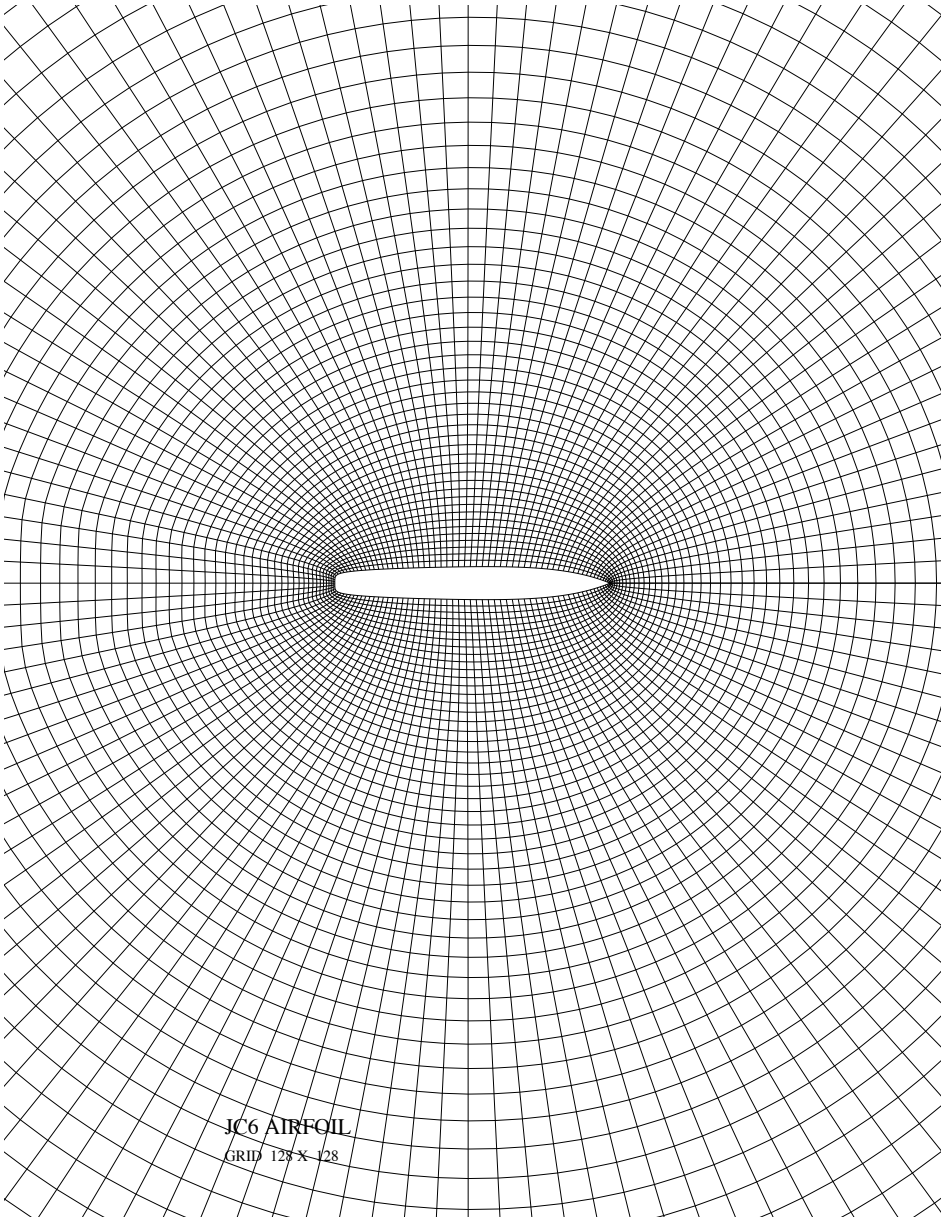

Figure 13. A size 128x128 O-topology mesh used for the JC6 airfoil. Each mesh element has an unit aspect ratio.

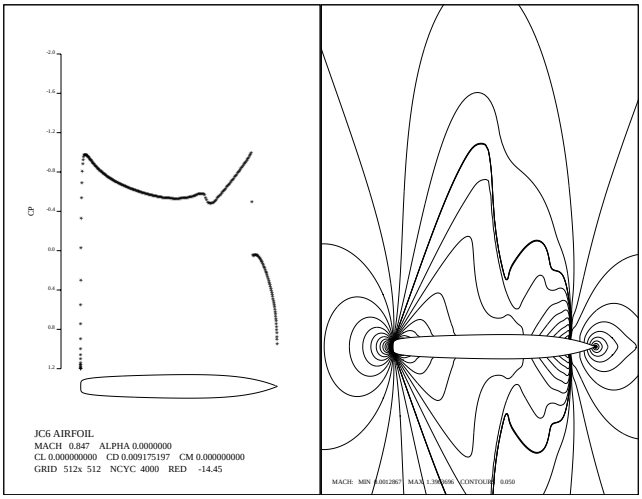

(a) Z-branch Cp Distribution and Mach Contours

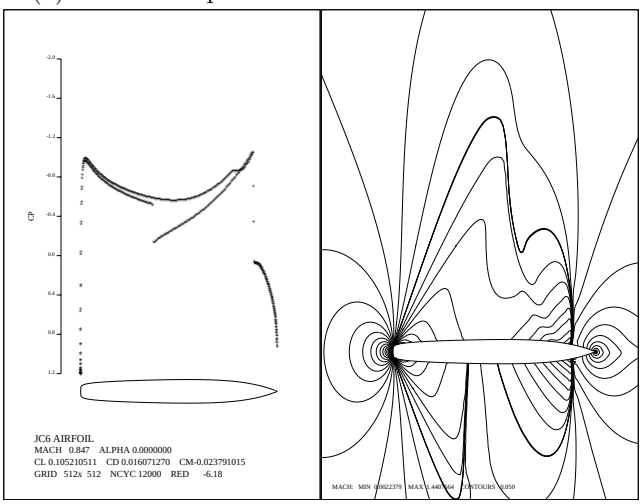

(b) P-branch Cp Distribution and Mach Contours

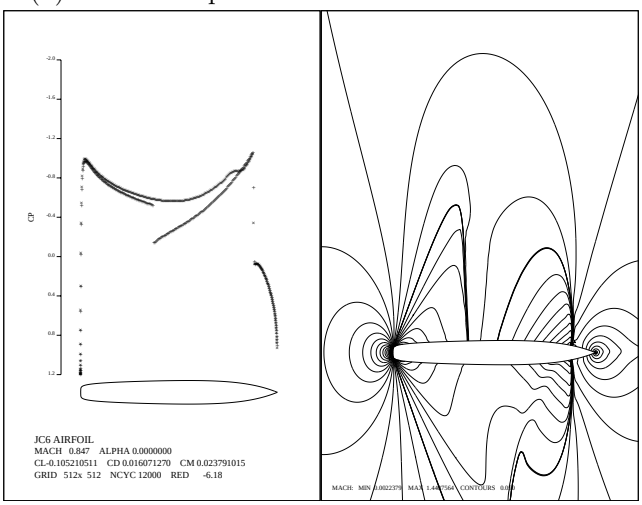

(c) N-branch Cp Distribution and Mach Contours

Figure 14. JC6 at Mach=0.847 showing (a) the z-branch solution, (b) the p-branch solution, and (c) the n-branch solution.

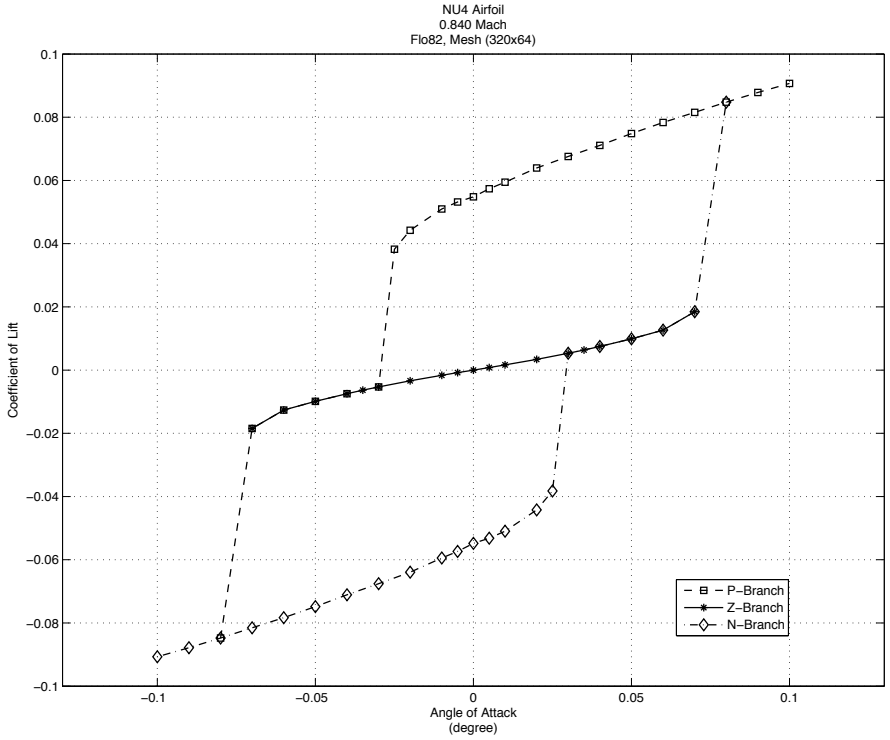

Figure 15. $C_L - \alpha$ **sweep for NU4 airfoil at Mach=0.840**

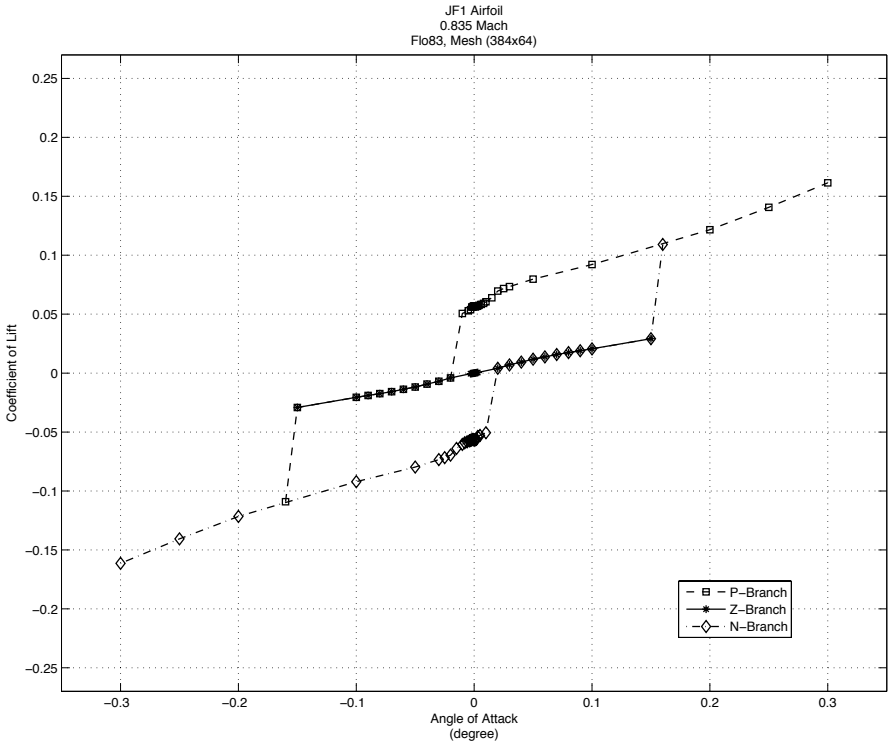

(a) Full view of the (a) $C_L - \alpha$ sweep curve

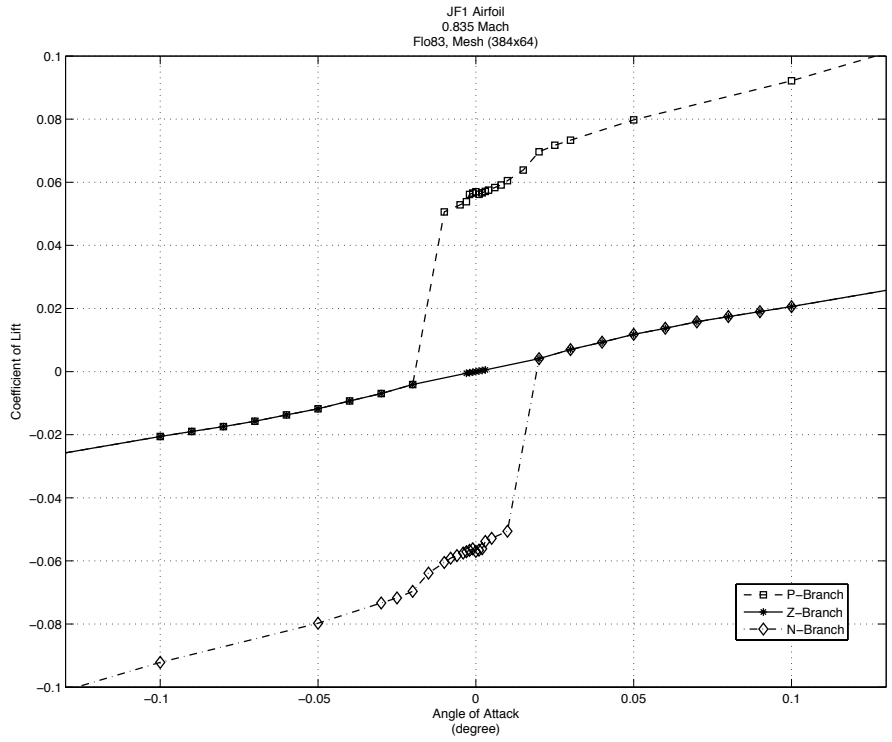

(b) Zoom of the (a) $C_L - \alpha$ sweep curve near the Z-branch

Figure 16. $C_L - \alpha$ sweep for JF1 airfoil at Mach=0.835. Top figure displays the full view. Bottom figure is a zoom near the Z-branch.

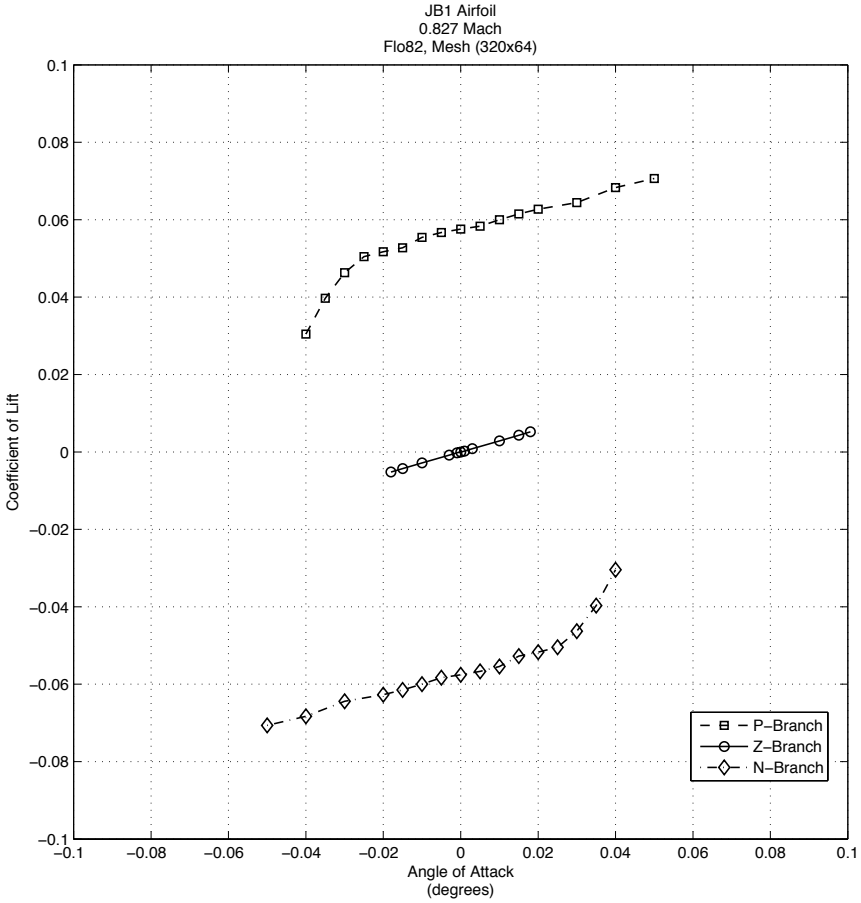

Figure 17. $C_L - \alpha$ **sweep for JB1 airfoil at Mach=0.827**

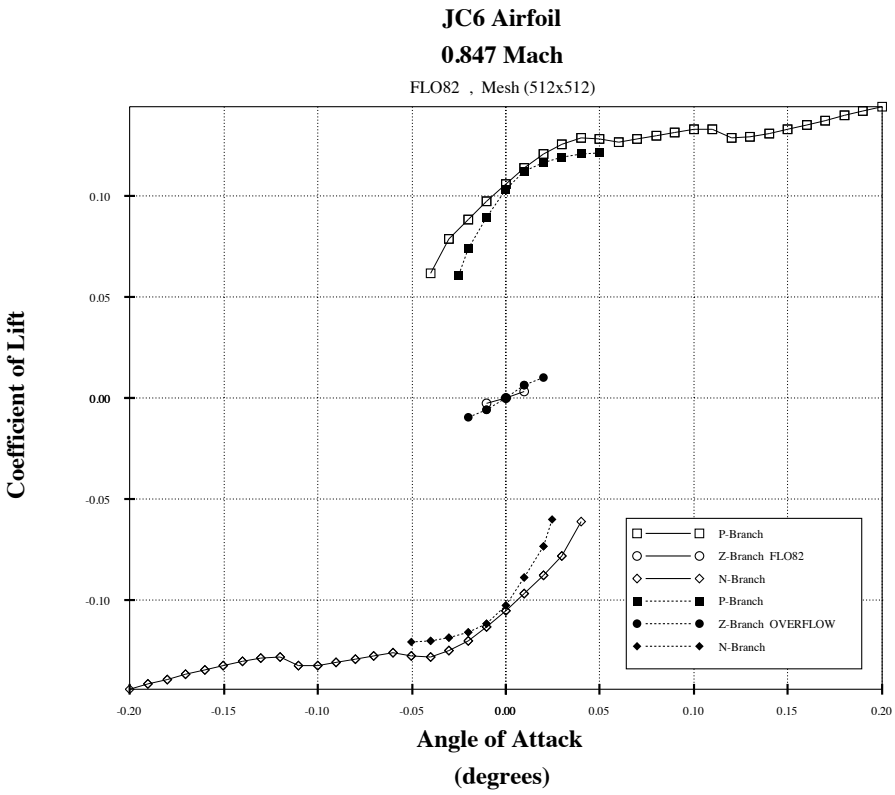

Figure 18. $C_L - \alpha$ **sweeps for JC6 airfoil at Mach=0.847.**